Hindawi
Journal of Chemistry
Volume 2021, Article ID 6663722, 15 pages
https://doi.org/10.1155/2021/6663722

Research Article

Comparison of CaO-NPs and Chicken Eggshell-Derived CaO in the Production of Biodiesel from *Schinziophyton rautanenii* (Mongongo) Nut Oil

Keene Carlvin Mmusi,[1,2] **Sebusi Odisitse**,[1] **and Florence Nareetsile**[3]

[1]*Botswana International University of Science and Technology, Department of Chemical and Forensic Sciences, Private Bag 16, Palapye, Botswana*
[2]*Botho University, Department of Applied Sciences, P O Box 501564, Gaborone, Botswana*
[3]*University of Botswana, Chemistry Department, Private Bag 0704, Gaborone, Botswana*

Correspondence should be addressed to Sebusi Odisitse; sebusi.odisitse@gmail.com

Received 5 October 2020; Revised 4 February 2021; Accepted 11 February 2021; Published 27 February 2021

Academic Editor: Francisco Javier Deive

The ever-increasing population growth and economic developments have heightened demand for energy. This has resulted in depletion and ever-rising prices of petroleum diesel, thus increasing environmental degradation. These complications have motivated this study for the search of an alternative eco-friendly and renewable source of energy such as biodiesel. Biodiesel has been found to be a potential alternative fuel for diesel. Biodiesel was produced by transesterification reaction of *Schinziophyton rautanenii* (mongongo) nut oil in the presence of a base heterogeneous catalyst: CaO derived from eggshell ash and synthesised CaO-nanoparticles (CaO-NPs). The catalysts were calcined at a temperature of 800°C for 3 h and characterized by scanning electron microscope-energy dispersive X-ray (SEM-EDX) where both catalysts showed agglomerated particles and high elemental composition of Ca and O. Powder X-ray diffraction (XRD) showed that CaO was present in both catalysts, and the average crystalline size obtained was 42 and 50 nm for CaO-NPs and eggshell ash, respectively. Fourier transmission infrared (FTIR) spectrometer showed absorption bands of CaO in both catalysts which were at 875 and 713.46 cm^{-1} for CaO-NPs and eggshell ash, respectively. The analysis of mongongo nut oil (MNO) and mongongo methyl esters (MMEs) was done according to the European biodiesel specification (EN 1421) and American Society for Testing and Materials (ASTM D675). Statistically, there was no significant difference between CaO-NPs and eggshell in terms of optimum yield ($P > 0.05$) using a sample *t*-test. However, in terms of catalyst loading, the eggshell was a better catalyst as it required a low catalyst load to obtain an optimum yield of 83% at 6 wt.% compared to CaO-NPs with an optimum yield of 85% at 12 wt.%. The reactions were all performed at constant reaction conditions of 9 : 1 methanol to oil ratio, 3 h reaction time, and 65°C reaction temperature.

1. Introduction

Ever since the revolution of industrialization, energy instability has been a challenging problem [1]. Globally scientists have been working hard in search of finding reliable, secure, clean, affordable, and sustainable energy resources [2]. Energy resources can be categorized into 3 major groups: fossil fuels, renewable, and fissile [3]. Biodiesel is one of the promising alternative sources of energy because it is a renewable source of energy. Fissile fuels are nuclear energy forms [4]. Fissile sources of energy include uranium and thorium. Renewable energy sources include biomass, hydro, wind, solar, marine, and hydrogen [5]. Fossil fuels are nonrenewable source of energy, and they have a negative impact on the climate through global warming [6]. Biodiesel has a high combustion efficiency, is biodegradable, acts as a lubricant, and it is sustainable and clean [7]. Biodiesel has attracted much needed attention as an alternative source of energy because of its easier accessibility [8]. Biodiesel is produced from triglycerides obtained from biological

sources. These include plants, vegetables, animal fats, waste oils, and microalgae. Researchers have reported different ways of producing biodiesel from waste vegetable oils using a transesterification method [9]. Some focused on (a) the effect of a catalyst such as heterogeneous catalyst, enzymatic catalyst, and homogenous catalyst; (b) effect of reaction time; (c) effect of temperature; and (d) the effect of alcohol used (mole ratio of alcohol to oil) [10–13].

Transesterification is a method used to produce alkyl esters (biodiesel) from oils/fats (triglycerides) in the presence of an alcohol and catalyst, as shown in Figure 1 [14]. The amount of catalyst is determined by the fatty acid present in the oil [15]. The process of transesterification involves a sequence of reversible reactions. The initial step involves the conversion of triglycerides to diglycerides; thereafter, diglycerides are converted to monoglycerides and lastly monoglycerides are converted to glycerol/glycerine [16].

A catalyst plays a major role in transesterification reaction. They are normally used in order to improve the rate of reaction, yield, and quality of biodiesel produced [18, 19]. Transesterification can be performed either by using homogenous, heterogeneous, or enzymatic catalyst [20, 21]. These catalysts can be classified into three (3) groups: acid catalyst, enzymatic catalyst, and base catalyst.

Homogeneous catalysts are normally used in commercial processes and exist in the same phase as the reactants. They are divided into acid catalysts (hydrochloric acid (HCl), sulphuric acid (H_2SO_4), sulfonic acid, and phosphoric acid) or basic catalysts (potassium hydroxide (KOH), potassium methoxide ($KOCH_3$), sodium hydroxide (NaOH), and sodium methoxide ($NaOCH_3$) [19, 20]. Homogeneous alkaline catalysts are more efficient as compared to homogenous acid catalysts and are a reason why they are the most preferred in the process of transesterification. The benefits of using these catalysts are that they are readily available and able to work at low temperatures and pressure [22]. Emeji reported a yield of over 95% using NaOH (0.5–2 wt.%) at a methanol oil molar ratio of 6 : 1 and temperature of 60–65°C [2]. Most oils contain fatty acids which cannot be converted into biodiesel using a base catalyst because of the production of soap which makes it difficult to separate the ester and glycerine [23]. Acid catalyzed transesterification does not produce soap or glycerol. It is also a single step reaction which enables transesterification with high free fatty acid (FFA) and water content. However, the reaction is slow; hence, it is less utilized especially in industrial processes [24].

Heterogeneous catalysts have gained a lot of recognition in recent years, as shown by a number of reports for the production of biodiesel [25]. Basic solid catalysts such as metal oxides, zeolites, and acidic solids are gradually becoming more popular due to the fact that they are noncorrosive and highly selective and have a prolonged life and cheaper manufacturing processes [26]. The benefit of using heterogeneous base catalysts is that they are easily separated from the product by filtration, and they can be recycled [27]. However, the limiting factor of using this catalyst is that the biodiesel feedstock should have a low FFA <3 wt.% and water content 1 wt.%. This is to avoid unfavourable reactions such as oil hydrolysis and saponification which tend to

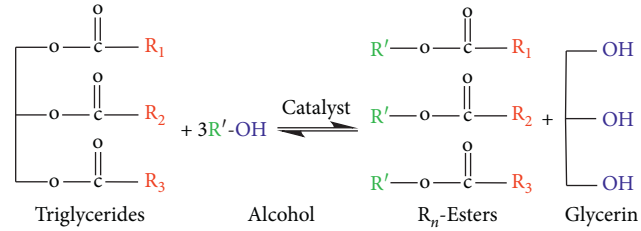

Figure 1: A typical transesterification reaction (drawn from [17]).

reduce the percentage biodiesel yield. Examples of heterogeneous catalysts are lanthanum oxide (La_2O_3), barium oxide (BaO), calcium oxide (CaO), calcium carbonate ($CaCO_3$), strontium oxide (SrO), and magnesium oxide (MgO) [28]. Acidic heterogeneous catalysts are suitable for the production of biodiesel due to their insensitivity to FFA and tolerance to the water content [29]. One of the benefits of using acid heterogeneous catalysts is that it can be easily removed from a mixture without affecting the catalytic activity. This catalyst is expensive as compared to the base heterogeneous catalyst. It operates at high temperatures, requires long reaction time, and high alcohol/oil mole ratio which may result in producing a low yield of biodiesel [17]. In recent studies, Nafion-NR50, sulfated zirconia, and tungstated zirconia have been used as acidic heterogeneous catalysts in the production of biodiesel [25, 30].

Lipases are the most utilized enzymes when it comes to using biological catalysts which can be extracted from plants, animals, and microorganisms such as *Mucor miehei* (*Lipozyme IM 60*), *Candida antarctia* (*Novozym 435*), *Pseudomonas cepacia* (*PS 30*), *Rhizopus oryzae*, *Penicillum expansum*, and *Bacillus subtilis* [18]. The benefits of using biocatalyst are that they produce higher yields, have better recovery of glycerol, are insensitive to high free fatty acids without saponification products (by product), and also, the process can be performed at low temperatures (up to 323 K) [31]. However, their limitations are that they are more expensive than chemical catalysts. The glycerol in the reaction mixture can cause reduction of the catalytic activity, resulting in a reduction of the biodiesel yield, slow reactions, and enzyme deactivation [32]. Also, enzymes are inherently slow compared to other catalyst and pH sensitive.

In this study, we used base heterogeneous catalysts, calcium oxide (CaO) derived from chicken eggshell ash, and calcium oxide nanoparticles (CaO-NPs) to produce biodiesel from mongongo nut oil (MNO). CaO has been the most utilized catalyst for the process of transesterification because it is easily prepared, has a high alkali pH value, and is insoluble in the reaction and nontoxic to the environment [33]. It is easily accessible as it can be found in chicken eggshell, ostrich eggshell, and meretrix Venus shell or is synthesised in the lab using materials that contain calcium carbonate [17, 24, 34]. Mongongo tree (*Schinziophyton rautanenii*) belongs to *Euphorbiaceae* family and the monotypic genus *Schinziophyton*. It is a large, deciduous tree which normally grows in sandy soils found from coast to coast in Southern Africa scattered around northern Namibia, southern Angola, Zambia, Botswana, Zimbabwe,

Mozambique, and Malawi. *Schinziophyton rautanenii* (shown in Figure 2(a)) is a multipurpose plant species found in Southern Africa with an ecosystem that provides a variety of goods and services. The fruits from these trees (shown in Figure 2(b)) are highly nutritious and rich in proteins and minerals. They also contain active antioxidants used for cosmetic and skin care products which have been consumed by the bushmen in the Kalahari desert in Botswana for over 7000 years [35]. It is identified by its large size and symmetric shape of its crown. Normally, the trees are densely populated in the area where they are found, and the seeds are readily available year round [7]. The seeds (shown in Figure 2(c)) are protected by a very hard and thick shell, and they make up to 70% of the fruit. Most rural communities in Southern Africa consider mongongo tree as an important source of food security and income [35]. The oil recovered from the seeds can be at most 60% which can be used for cooking, cosmetic application, fuel, and medicinal purposes, and the protein content from the nuts is about 30%, while the leaves can be used as animal feed [36]. Even though mongongo oil is used for making cosmetic and skin care products and also as a source of food, not much work has been done on the production of biodiesel using mongongo oil.

The study is therefore focused on preparation and characterization of heterogeneous catalysts and their catalytic behaviour towards the production of biodiesel from *Schinziophyton rautanenii* (mongongo) nut oil (MNO).

2. Materials and Methods

2.1. Materials. Methanol 99.5%, ethanol 95%, hydrochloric acid (AR Grade) 38%, magnesium carbonate (AR Grade), and *n*-hexane were purchased from SkyLabs. Potassium hydroxide 99%, diethyl ether 99.5%, sodium hydroxide pellets 99%, and calcium nitrate tetrahydrate 99% were purchased from Rochelle Chemicals. Chloroform 99%, sodium thiosulphate 99%, 99.8% phenolphthalein, 99.8% iodine, 95% petroleum ether, and 99% potassium iodide were purchased from Sigma-Aldrich.

2.2. Collection and Preparation of Mongongo Nut Oil. Mongongo (*Schinziophyton rautanenii*) nuts were collected from the surroundings of a village called Ukuse, near Shakawe in the northwest region of Botswana. The chicken eggshells were collected from the cafeteria at Botswana International University of Science and Technology (BIUST) located in the northern part of Botswana, while CaO-nanoparticles were prepared in the laboratory.

Mongongo nut oil (MNO) was extracted traditionally by crushing the nutshells with a stone to remove the nuts from inside. The nuts were then boiled in a pot with water to moisten the layer covering the nuts and making it easy to remove. Thereafter, the nuts were crushed until a sticky nut paste was produced. The paste was placed back into the pot with boiling water and heated gently. Boiling was continued for some time to allow water evaporation and decantation of the oil. The oil was then allowed to cool and thereafter poured in the bottles for storage.

2.3. Preparation of Catalysts

2.3.1. Chicken Eggshell. Eggshells were washed three (3) times with distilled water to remove dirt and contaminants. The shells were oven-dried for 24 h at a temperature of 100°C and then crushed using a mechanical pulveriser into fine particles of 100 μm. The fine powdered eggshells were then calcined at a temperature of 800°C for 3 h using a Carbolite AAF 1100 furnace to convert $CaCO_3$ into CaO. The chemical reaction of the process is shown as follows:

$$CaCO_3 \xrightarrow{\Delta} CaO_{(s)} + CO_{2(g)} \quad (1)$$

The ash was used as a heterogeneous catalyst for the conversion of mongongo nut oil into mongongo methyl esters (biodiesel) by a transesterification reaction. The method used was adapted from Tshizanga [17].

2.3.2. Synthesis of CaO-Nanoparticles. 10.0 g of calcium nitrate tetrahydrate was accurately weighed and dissolved in 100 mL of distilled water. A solution of sodium hydroxide was made by dissolving 3.3 g of the pellets in distilled water. This solution was added to calcium nitrate tetrahydrate solution dropwise while vigorously stirring the solution at room temperature. A white precipitate of calcium hydroxide was filtered, washed with warm distilled water, and oven-dried for 24 h at a temperature of 80°C. The dried calcium hydroxide was converted into calcium oxide nanoparticles (heterogeneous catalyst) by calcination at a temperature of 800°C using a carbolite AAF 1100 furnace for 3 h. The chemical reactions of this process are shown in the following equations:

$$Ca(NO_3)_{2(l)} + 2NaOH_{(s)} \xrightarrow{\text{Stirring}} Ca(OH)_{2(s)^+} + 2NaNO_{3(l)} \quad (2)$$

$$Ca(OH)_{2(s)} \xrightarrow{\Delta} CaO_{(s)} + H_2O_{(g)} \quad (3)$$

2.4. Catalyst Characterization

2.4.1. Powder X-Ray Diffractometer (XRD). Powder XRD in this study was used to characterize the catalysts: eggshell ash and calcium oxide nanoparticles (CaO-NPs), by identifying the elemental composition and calculating the size of particles. It was used to acquire qualitative analysis investigating the elemental and structural materials of the eggshell ash-derived CaO and CaO-NPs. A Bruker D8 Advance from Billerica, United States of America, was used to identify crystalline phase in the samples, determine the crystalline size, and shape from the diffraction peaks. This instrument comes with EVA and TOPAS software used to analyse data with an operating current and voltage of 40 mA and 40 kV, respectively.

2.4.2. Scanning Electron Microscope-Elemental Dispersion X-Ray (SEM-EDX). The morphological and elemental analysis of the catalysts: chicken eggshell ash-derived CaO

Figure 2: Photographic images of mongongo tress (a), mongongo fruit (b), and mongongo nuts (c).

and CaO-NPs were obtained using a Scanning Electron Microscope coupled with an Elemental Dispersion X-ray. The prepared catalysts and catalyst support were placed on a stub and coated with gold in a sputtering device before being observed by Jeol JSM-7100F from Tokyo, Japan. The elemental dispersion X-ray was used to provide information on qualitative and quantitative analysis of elements present in the catalyst. This instrument captures images of samples by scanning it with a focused beam of electrons. The electrons interact with atoms in the sample, giving out various signals which have information about the sample's surface topography and composition.

2.4.3. Fourier Transmission Infrared Spectroscopy (FTIR). FTIR was used to identify the functional groups present in mongongo nut oil (MNO) and MMEs. Characterization was also performed on the catalysts: eggshell ash and CaO-NPs. The functional groups were recorded from the region of 4000 to 400 cm^{-1} using a PerkinElmer System 2000 FTIR spectrometer from Waltham, United States of America.

2.5. Determination of Physicochemical Properties of MNO/MMEs

2.5.1. Saponification Value. A solution of potassium hydroxide (14.2 g, 0.5 M) was prepared in 10 mL of distilled water. The solution was made to the mark with 95% ethanol in a 500 mL volumetric flask. The solution was left for 24 h before decanting. Thereafter, 25 mL of the solution was titrated against 0.5 M hydrochloric acid using phenolphthalein indicator, and the values were recorded as a blank. 2.0 g of MNO/MMEs and 25 mL of alcoholic potassium hydroxide were added into 250 mL round-bottom flask. The solution was heated and refluxed for 1 h in a steam bath with continuous stirring. Thereafter, phenolphthalein indicator was added, while the solution was still hot, and the excess potassium hydroxide was titrated with 0.5 M hydrochloric acid until a cloudy solution was formed. The method was adopted from Tesfaye et al. with modifications, and the saponification value was calculated using the following equation [37]:

$$\text{saponification value} = \frac{56.1\,(b-a)\times N}{W}, \tag{4}$$

where b = blank titre value (mL), a = sample titre value (mL), N = normality of hydrochloric acid (N), and W = weight of sample (g)

2.5.2. Acid Value. 2.5 g of MNO/MMEs and 50 mL of 95% ethanol were added into a 250 mL conical flask. Four (4) drops of phenolphthalein indicator were added to the mixture. The solution was titrated against 0.5 M potassium hydroxide until the first pink colour appeared and visible for 30 sec. According to American society for testing and materials (ASTM D974), acid value and free fatty acid value are calculated using equations (5) and (6), respectively [17]:

$$\text{acid value} = \frac{56.1\times V\times N}{W}, \tag{5}$$

where V = volume of standard potassium hydroxide (mL), N = normality of the potassium hydroxide solution or sodium hydroxide solution (N); and W = weight of the sample (g); hence, the free fatty acid is calculated with equations (2) and (3):

$$\text{free fatty acid (FFA)} = \frac{\text{acid value}}{2}. \tag{6}$$

2.5.3. Peroxide Value. In a 250 mL conical flask, 5.0 g of MNO/MMEs and 30 mL of mixture of acetic acid and chloroform solvents (3 : 2) were added and gently swirled. 1 mL of potassium iodide solution was added to the solution and kept for 1 min in the dark room with occasional shaking, and then, 30 mL of distilled water was added. Then liberated iodine was slowly titrated against sodium thiosulphate solution with vigorous shaking until a yellow colour was not visible. 1 mL of starch solution indicator was added to the conical flask and then continued titrating with vigorous shaking (to realise all I_2 from CH_3Cl layer) until all the blue colour disappeared. The method used was adapted from Tesfaye and Abebaw, and the peroxide value was calculated using the following equation [37]:

$$\text{peroxide value (PV)} = \frac{V \times N \times 100}{W}, \quad (7)$$

where V = volume of sodium thiosulphate (mL), N = normality of hydrochloric acid (N), and W = weight of sample (g).

2.5.4. Iodine Value. In a 250 mL conical flask, 200 mL of mixed solvents of cyclohexane and acetic acid (1 : 1 ratio) was prepared. 0.13–0.15 g of MNO/MMEs, 20 mL of the prepared solvent mixture of cyclohexane and acetic acid, and 25 mL of Wij's reagent were added into 250 mL conical flask. The flask was placed in a dark room for 1 h. The iodine value was determined according to the European standard (EN 1411) by titration using sodium thiosulphate [1, 38]. The following equation was used to calculate the iodine value:

$$\text{iodine value (IV)} = \frac{(b - a) \times N \times 1.269 \times 100}{W}, \quad (8)$$

where b = blank titre value (mL), a = sample titre value (mL), N = normality of thiosulphate (N), and W = weight of sample (g).

2.5.5. Density. The Atago densimeter was used to measure densities of MNO, and MMEs were determined using density meter. The MNO and MMEs were injected into the density meter using a syringe, and densities were recorded at temperatures of 40 and 100°C [30, 39].

2.5.6. Refractive Index. An Anton Paar refractometer was used to determine the refractive index of MNO and MMEs. About 1 mL (1 drop) of MNO/MMEs was placed in the instrument at room temperature, and the value was recorded.

2.5.7. Kinetic Viscosity. A U-Visc 210/220 automatic viscometer was used to determine the kinematic viscosity of MNO and MMEs. About 10 mL of the sample was drawn into viscometer tubes and placed onto the auto sampler. The viscometer tubes were placed at different oil baths at temperatures of 40 and 100°C. The method was performed according to American society for testing and materials (ASTM D445:19) [17].

2.6. Transesterification Reaction. Transesterification method was employed to produce biodiesel using a mole ratio of 9 : 1 methanol to oil for the reaction. 10.0 g of MNO was added into a 250 mL round-bottomed flask. The contents were then heated under reflux to a temperature between 65 and 70°C in a water bath until the oil and water bath temperature reached equilibrium. A mixture of methanol and the catalyst was made in a beaker and stirred until homogeneity was reached. Once the oil had reached a temperature between 65 and 70°C, a mixture of methanol and the catalyst was added to the round-bottomed flask. The mixture was continuously stirred at a temperature of 65°C for 3 h. The mixture was then transferred into a separatory funnel and allowed to stand for phase separation. After phase separation, glycerol (lower layer) was removed and only the ester mixture (top layer) was left in the separating funnel. The ester mixture was washed with warm distilled water to remove traces of the catalyst and alcohol until the water layer was clear. Anhydrous magnesium carbonate (drying agent) was added to get rid of any water left in the methyl ester. The method was adopted from Mirghiasi et al. with modifications [40]. The percentage yield of the methyl esters obtained was calculated as follows:

$$\%\ \text{yield FAMEs} = \frac{\text{weight of FAMEs produced (g)}}{\text{weight of MNO for reaction (g)}} \times 100. \quad (9)$$

2.7. Gas Chromatography-Mass Spectrometer (GC-MS) Analysis. The methyl esters from biodiesel were analysed using gas chromatography mass spectrometer which was equipped with a NIST library for identification of peaks. The analysis was carried using Agilent 7890A Gas Chromatograph (Agilent Technologies, Santa Clara, United States of America) with an Agilent 5975C Mass Spectrometry Detector (Agilent Technologies) and an Agilent 7693 auto sampler (Agilent Technologies). The separation was achieved on a HP-5MS 5% phenyl methyl silox column (30 m × 250 μm × 25 μm). Approximately 1 mL of sample solution was diluted with 1 mL of hexane and then placed in the auto sampler sample rack for injection in a split ratio of 80 : 1. The parameter settings for the GC-MS are displayed in Table 1.

3. Results and Discussion

3.1. Characterization of Chicken Eggshell Ash and CaO-Nanoparticles

3.1.1. Powder X-Ray Diffraction (XRD) Analysis. The powder X-ray diffraction (XRD) was used to analyse chicken eggshell and chicken eggshell ash-derived CaO samples. The measurements were performed at 2θ from 0° to 90°. The powder XRD pattern of the eggshell ash-derived CaO and eggshell shown in Figure 3 was identified as CaO and $CaCO_3$, respectively. CaO matched with PDF 04-007-9734 (refer to Supplementary Data Section 1.1: Figure 1) was successfully formed after calcination with no traces of

Table 1: GC-MS parameters for the analysis of biodiesel.

Parameter	Setting
Column temperature program	325°C/min
Run time	35.5 min
Injector temperature	290°C
Total flow	84 mL/min
Injection volume	1 μL
Split flow	80 mL/min
EM volt	1082 V

$CaCO_3$ proving that the eggshell ash produced pure CaO. The results could also imply that the eggshell ash obtained was completely crystallized because of the removal of CO_2 during the thermal treatment process. The successful transformation of $CaCO_3$ to CaO is seen in the power XRD pattern in Figure 3 of the chicken eggshell ash-derived CaO calcined at 800°C and eggshell, and the results are similar to those reported by Hua et al. [34]. The estimated average particle size of the chicken eggshell ash-derived CaO was calculated to be 50 nm (with $k = 1$).

Figure 4 shows the powder XRD pattern of calcined CaO-NPs at 800 and 900°C. The powder XRD pattern of CaO-NPs shows sharp and separated peaks indicating that CaO was produced from $Ca(OH)_2$. Mirghiasi et al. also observed similar patterns [40]. The spectrum of CaO-NPs calcined at 800°C shows higher peaks than that of CaO-NPs calcined at 900°C, indicating that it has a high degree of crystallinity [41]. CaO-NPs sample calcined at 800°C matched with COD 9006694 (refer to Supplementary Data Section 1.2: Figure 2) was chosen to be used in the production of biodiesel from mongongo nut oil because it had more of CaO and it was expected that it would give a better yield compared to the sample calcined at 900°C.

3.1.2. Fourier Transform Infrared Spectroscopy (FTIR) Analysis. FTIR spectrophotometer was used to determine characteristic bands of the chicken eggshell ash-derived CaO and eggshell, and the spectra are shown in Figure 5. Figure 5(a) which is a spectrum of the chicken eggshell shows a sharp peak at 3614.37 cm^{-1} which was due to the presence of hydroxyl (–OH). Witoon reported similar results of the broad (–OH) stretch vibration [42]. The presence of the stretch vibration was assumed to be due to the adsorption of atmospheric water [43]. The band observed at 1083.86 cm^{-1} is due to the presence of $CaCO_3$ [41]. Figure 5(b) shows chicken eggshell ash-derived CaO calcined at 800°C with two bands at 1405.93 and 873.64 cm^{-1} which indicate the presence of C-O bond. Chicken eggshell was heated at high temperatures (800°C) during calcination resulting in the loss of $CaCO_3$, hence reducing the mass of the functional groups bonded to the CO_3^{2-} ions and the intensity of $CaCO_3$ peaks [34]. The strong band observed at 713.46 cm^{-1} is due to the (Ca-O) bond, and it is consistent with literature values [44, 45]. The presence of these characteristic bands indicates that CaO was produced.

The FTIR spectra of the CaO-NPs and $Ca(OH)_2$ are shown in Figure 6. $Ca(OH)_2$ was thermally decomposed at

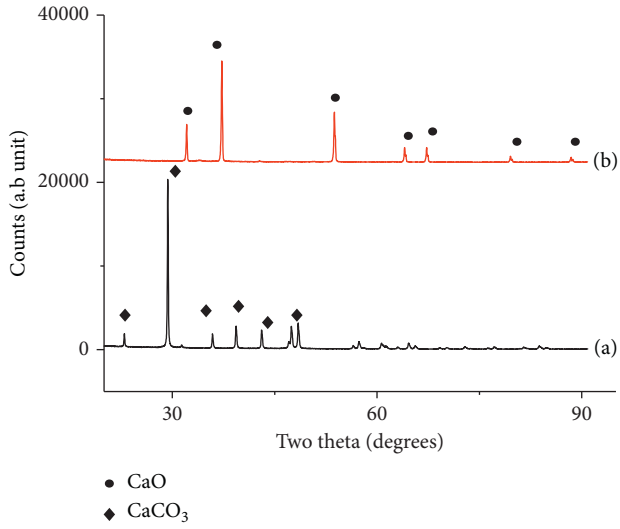

Figure 3: XRD pattern of samples: (a) chicken eggshell (black); (b) chicken eggshell ash-derived CaO calcined at 800°C (red).

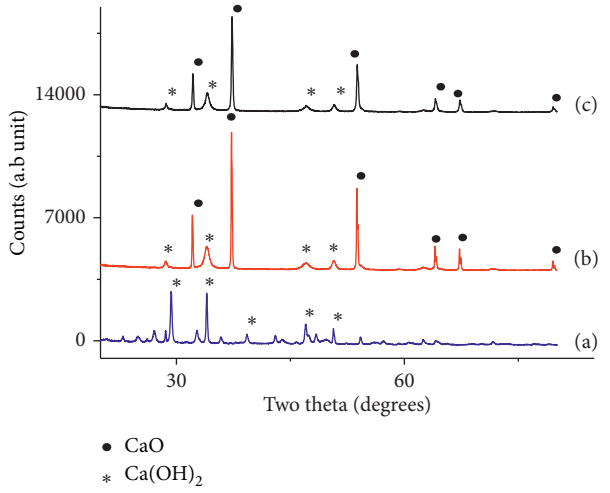

Figure 4: XRD pattern of samples: (a) $Ca(OH)_2$ (blue); (b) CaO-NPs calcined at 800°C (red); (c) CaO-NPs calcined at 900°C (black).

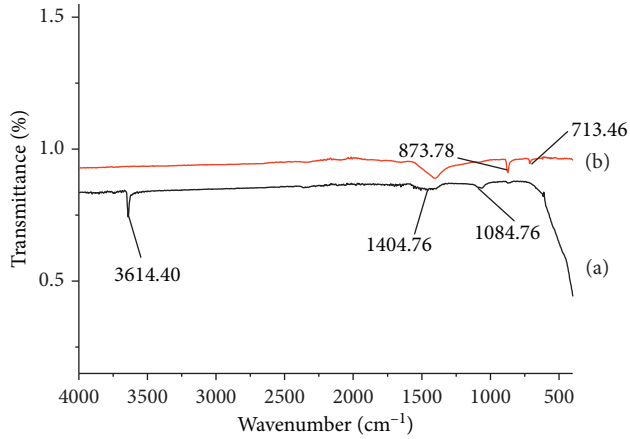

Figure 5: FTIR spectra of (a) chicken eggshell (black) and (b) chicken eggshell ash-derived CaO calcined at 800°C (red).

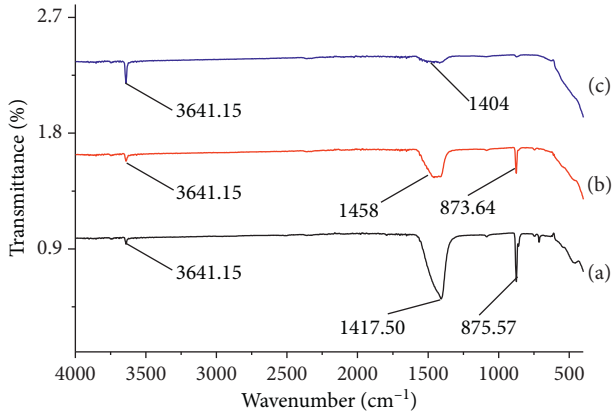

Figure 6: FTIR spectra of (a) $Ca(OH)_2$ (black), (b) CaO-NPs calcined at 800°C (red), and (c) CaO-NPs at 900°C (blue).

800 and 900°C to produce CaO-NPs. Calcination at 900°C clearly shows a sharp absorption peak at 3641.15 cm^{-1} associated with the hydroxyl (–OH) stretching group [40]. A peak observed at 1404 cm^{-1} is indicative of the presence of (C-O) bond. Similarly, a low intensity peak assigned as the (–OH) stretching group is also observed in CaO-NPs calcined at 800°C (Figure 6(b)) at 3641.15 cm^{-1}. At 800°C, spectra show peaks at 1458 and 873 cm^{-1} and these are associated with the (C-O) bond. The hydroxyl (-OH) stretching vibration shown at both 800 and 900°C may be due to adsorption of water to CaO from the atmosphere during sample handling [46]. According to reports by Elmastaş et al. and Harsh-Hebbar et al., CaO exposed to open air for a long period of time can be hydrolyzed to $Ca(OH)_2$ [45, 47]. The other reason could be that some of the $Ca(OH)_2$ may have not been completely transformed to CaO, and thus, some of the hydroxide ions (–OH) remained [48]. The peaks observed at 1458, 1470, and 1404 cm^{-1} are associated with the (C-O) bond, indicating the calcination of $Ca(OH)_2$ to produce CaO-NPs [49]. The observed bands at 875 and 873 cm^{-1} are due to the (Ca-O-Ca) bonds, and these were also reported by Anantharaman and coworkers also observed [50].

3.1.3. Scanning Electron Microscope-Elemental Dispersive X-Ray (SEM-EDX) Analysis. Figure 7 shows the SEM images of CaO from chicken eggshell ash calcined at 800°C. Figure 7(a) shows granular and irregular particles indicating the formation of CaO particles. These agglomerated particles are similar to those observed by Fayyazi et al. [51]. The particles appear to be clustered due to the exposure to high temperatures during calcination [52]. Small particles are observed because large amounts of CO_2 gas escaped during calcination (800°C) when $CaCO_3$ was decomposed to CO_2 and CaO [53]. Supriyanto et al. reported similar results showing that exposure to high temperatures results in chicken eggshell ash-derived CaO having more porosity than eggshell due to the release of CO_2 [54]. The SEM image in Figure 7(b) shows interconnected particles of irregular shapes and sizes and tiny crystals embedded in the particles caused by the heterogeneous arrangement in the mechanical properties of the sample which plays a significant role in the activity of the catalyst [24, 55]. Figure 8 shows the spectrum of chicken eggshell ash-derived CaO which indicates that CaO was indeed formed in high concentration as expected. The results are similar to those reported by Chung et al. and Syazwani et al. [10, 56]. The percentage atomic compositions were obtained as 28.15, 64.40, 16.24, and 0.01% for calcium (Ca), oxygen (O), carbon (C), and magnesium (Mg), respectively. The results are indicative of the presence of CaO in the eggshell ash.

Figure 9 shows the SEM images of CaO-NPs calcined at 800°C. Figure 9(a) shows particles that are agglomerated suggesting that these particles are porous in nature [57]. Figure 9(b) shows particles arranged in a grain-like structure with a spherical morphology. The individual particles were nano-sized crystals similar to that found in literature [44, 58]. The elemental composition of CaO-NPs shown in Figure 10 indicates that CaO was formed in high concentration. The percentage atomic compositions were obtained as 38.18, 45.56, 6.05, and 0.01% for calcium (Ca), oxygen (O), carbon (C), and magnesium (Mg), respectively. The results indicate that indeed CaO has been produced.

3.2. Characterization of Mongongo Nut Oil and Methyl Esters (Biodiesel)

3.2.1. Physicochemical Properties of Mongongo Nut Oil and Its Biodiesel. All oils have unique physical, chemical, and compositional parameters. This work describes some important properties of mongongo nut oil (MNO) and its resultant biodiesel. The properties studied are as follows: kinematic viscosity, density, acid value, iodine value, peroxide value, saponification value, free fatty acid, and refractive index. Table 2 shows the physicochemical properties of MNO and MMEs from chicken eggshell ash-derived CaO and CaO-NPs in comparison to the European biodiesel specification (EN 1421) and American society for testing and material (ASTM D675) which are the standard set for biodiesel. Having considered the information presented in Table 2 for MNO and MMEs (chicken eggshell ash-derived CaO and CaO-NPs), it is observed that MNO had a kinematic viscosity of 88.14 and 9.676 mm/s^2 at temperatures of 40 and 100°C, respectively. Kinematic viscosity was measured at different temperatures which are normally found in a diesel engine during operation. The kinematic viscosity for MMEs recorded was 6.38 and 5.94 mm/s^2 for chicken eggshell ash-derived CaO and CaO-NPs, respectively. Furthermore, the kinematic viscosity recorded for MMEs was 2.36 and 1.32 mm/s^2 for chicken eggshell ash derived and CaO-NPs catalyst at 40 and 100°C, respectively. The kinematic viscosity recorded for the chicken eggshell ash-derived CaO catalyst was slightly above the recommended set limit by ASTM D6751-09. The kinematic viscosity could have been high due to the fact that the oil was not taken for pretreatment method before transesterification reaction, in which Woo and Kim reported that it lowers the kinematic viscosity of the biodiesel [59]. It is very important to have a low kinematic viscosity for biodiesel because high kinematic

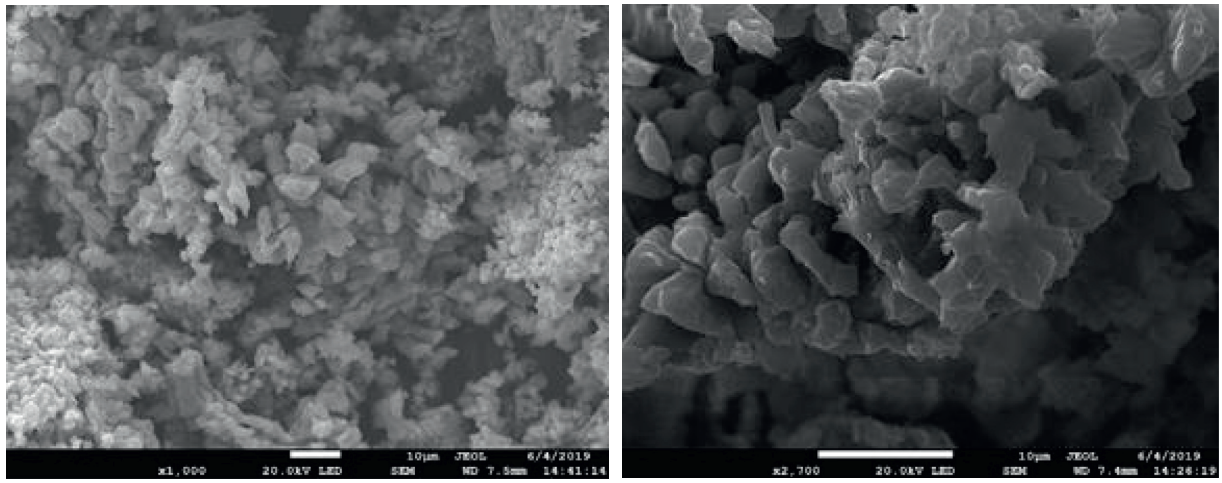

Figure 7: SEM images of chicken eggshell ash-derived CaO which were calcined at 800°C.

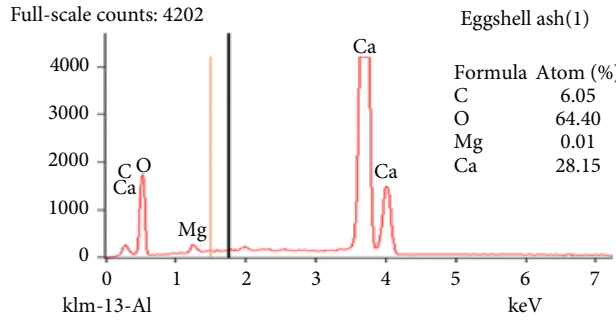

Figure 8: SEM-EDX spectrum of chicken eggshell ash-derived CaO which were calcined at 800°C.

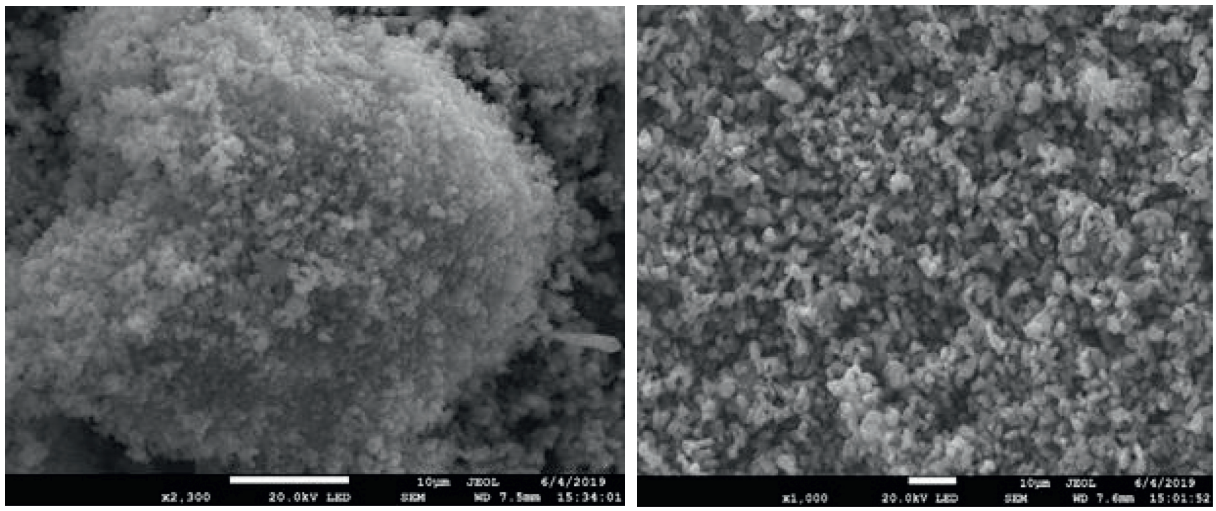

Figure 9: SEM images of CaO-NPs which were calcined at 800°C.

viscosity can cause problems in the diesel engine such as poor atomization during spray. High viscosity also requires more energy from the fuel atomization and also increases the carbon deposits [60]. However, extremely low viscosities may have implications because required lubrication may not be delivered at the pumps and injector plungers. They can also form abnormalities and cause leakages in the injector and injector pumps which may result in accumulation of small or no fuel in the engine to produce power [21]. The values of the kinematic viscosity recorded are within range or close to those of the set biodiesel standards and similar to those found in literature [61]. Density is a very important parameter. It plays a significant role in the properties and characteristics of fuel quality in determining the energy of

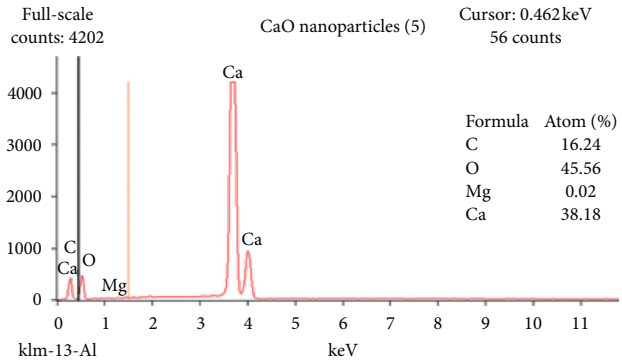

Figure 10: SEM-EDX analysis of CaO-NPs which were calcined at 800°.

Table 2: Physiochemical properties of mongongo nut oil and its methyl esters from eggshell ash and CaO-NPs.

Properties	MNO	MMEs (chicken eggshell ash-derived CaO)	MMEs (CaO-NPs)	Diesel[c]	Standards for biodiesel
Viscosity (40°C), mm^2/s	88.14	6.38	5.94	3.23	1.9–6.0[a] 3.5–5.0[b]
Viscosity (100°C), mm^2/s	9.676	2.36	1.32	1.24	N/A
Density (15°C), kg/m^3	928	892	889	845	860–900[b]
Density (40°C), kg/m^3	911	877	864	824	N/A
Acid value, mg KOH/g	1.12	0.46	0.43	N/A	0.5 (max)[b] 0.8 (max)[a]
Iodine value, $I_2/100$ g	30.47	24.35	17.01	N/A	120 (max)[b]
Peroxide value, mEq/kg	0.73	0.61	0.59	N/A	2.0 (max)[b]
Saponification value, mg KOH/g	184.56	231.41	253.53	N/A	N/A
Free fatty acid, %	0.6	0.23	0.21	N/A	1[b]
Refractive index (25°C)	1.4890	1.4826	1.4821	N/A	N/A

[a]Biodiesel (B100) Fuel Quality Standard ASTM D6751-09 [73]; [b]Atabani et al. 2014 [74]; [c]EN 14214 standard for biodiesel [36].

the biodiesel [62]. The density of MNO was successfully reduced from 928 to 892 kg/m^3 for MMEs with chicken eggshell ash-derived CaO and 889 kg/m^3 for MMEs with CaO-NPs at 15°C. The MME values recorded were within the standard set limit of EN 14214 for biodiesel. Furthermore, density was investigated at 40°C, and density of MNO was reduced from 911 to 877 and 864 kg/m^3 for MMEs with chicken eggshell ash-derived CaO and MMEs with CaO-NPs, respectively. Canesin et al. performed a similar work on methyl esters from different oils, and the densities observed were ranged between 871 and 880 kg/m^3 [63]. The kinematic viscosity and density measured are within the set biodiesel standards and indicate that biodiesel produced from MNO may find use as biofuel.

MNO gave an acid value of 1.12 mg KOH/g which is lower than the value reported by Cheikhyoussef et al. (2.44 mg KOH/g). This variation may be due to fact that the oils were collected from different regions. The environment and climatic conditions could also play a role in the composition of the oil [7]. MMEs were also investigated for acid value from the use of both chicken eggshell ash-derived CaO and CaO-NPs as catalysts, and the acid values obtained were 0.46 and 0.43 mg KOH/g, respectively. This remarkable reduction of acid value from MNO indicates that the MMEs may have a potential to give outstanding atomization in the diesel engine [64]. The values obtained are satisfactory as they are below the limit of 0.5 and 0.8 mg KOH/g according to EN 14214 and ASTM D6751 standards, respectively. FFA value for MNO was 0.6%, while FFA values obtained for MMEs were 0.23 and 0.21% using chicken eggshell ash-derived CaO and CaO-NPs, respectively. FFA values obtained for MNO and MMEs are satisfactory because both are all below 1%, and in this case, the alkali transesterification method is suitable to produce biodiesel. Moreover, oil with high FFA has been reported to produce excessive amount of soap which interferes with the separation and washing process of biodiesel after the reaction by forming emulsions which may result in loss of yield [65].

The iodine value was determined on MNO and MMEs, and the iodine value obtained for MNO was 30.47 $I_2/100$ g, while for MMEs were 24.35 and 17.01 $I_2/100$ g using chicken eggshell ash-derived CaO and CaO-NPs catalyst, respectively. The results obtained for MMEs are satisfactory as the values are lower than the set standard limit for biodiesel by EN 14214. Rao et al. indicated that the lower the iodine value, the better the fuel quality, and a high value is an indication for a high potential for the degradation of biodiesel [66]. A peroxide value was determined through iodometric titration, a commonly used method which is fast and affordable. This parameter is used to determine the availability of primary and secondary oxidation products in biodiesel [67]. MNO gave a peroxide value of 0.73 mEq/kg, which is significantly lower than 3.98 mEq/kg reported by Cheikhyoussef et al. [7]. The value obtained for MMEs using chicken eggshell ash-derived CaO catalyst was 0.61 mEq/kg, while for CaO-NPs catalyst was 0.59 mEq/kg [77]. These values are within

the set limit of 2.0 mEq/kg; hence, they are satisfactory [7]. Saponification value is mainly used to investigate adulterations in fuel. The value obtained for MNO was 184.56 mg KOH/g. It is similar to the saponification value of MNO (185 mg KOH/g) reported by Mabaleha et al. and Mitei et al. obtained values ranging between 184 and 189 mg KOH/g [68, 69]. High saponification value in oil is an indication of high presence of fatty acids which may lead to soap formation during transesterification. This could result in low yield, and it may become complex to separate the biodiesel from glycerol [70]. The values for MMEs were 231.41 and 253.53 mg KOH/g for chicken eggshell ash-derived CaO and CaO-NPs catalysts, respectively. This implies that 231 and 253 mg KOH/g are needed to saponify 1 g potassium hydroxide. The increase in saponification value of MMEs was expected because of the increase in number of the ester bonds in the FAMEs compared to MNO, and thus, the results indicate that MMEs have been produced [71]. Refractive index is a useful fluid characteristic magnitude used to investigate the purity of the fuels [72]. The refractive index was also measured for MNO and MMEs at room temperature. MNO gave a refractive index of 1.4890 which is similar to the refractive index of 1.48 reported by Cheikhyoussef, and there was a successful reduction to 1.4826 and 1.4821 in MMEs for chicken eggshell ash-derived CaO and for CaO-NPs catalysts, respectively [6]. Just as explained in iodine value, the reduction in the degree of unsaturation improves the quality of the biodiesel. Therefore, in this case, the results obtained show a remarkable reduction for refractive index of MNO to MMEs, indicating that the biodiesel produced could be of good quality.

3.2.2. Transesterification of Mongongo Nut Oil to Biodiesel. The chromatogram shown in Figure 11 shows the peaks identified for the fatty acid methyl esters with their retention times using chicken eggshell ash-derived CaO. According to the results, the GC-MS method employed gave a total of 7 major peaks, which corresponded to the different ester groups. The FAMEs identified in order of their retention times were palmitic acid methyl ester (15.93 min), linoleic acid methyl ester (18.23 min), linoleic acid methyl ester (18.29 min), steric acid methyl ester (18.61 min), linolelaidic acid methyl ester (20.25 min), linolelaidic acid methyl ester (20.85 min), and linoleic acid methyl ester (23.59 min).

The results of the FAMEs found are similar to those reported by Gebreyohans for the production of biodiesel from jatropha seed oil [30]. The FAME results show that the methyl esters can be produced from MNO using chicken eggshell ash-derived CaO as a catalyst. However, the compounds found in this biodiesel are a mixture of ethers, acid esters, and esters. These classes of saturated fatty acids improve fuel properties such as kinematic viscosity, density, acid value, and also peroxide value of the produced biodiesel as reported in the literature [75, 76]. This is so because these classes of compounds have generally low kinematic viscosity and density as a result of transesterification reaction and also being stable with regard to oxygen susceptibility [77–79]. These are some of the physicochemical parameters that improve the quality of the biodiesel and are also the most monitored parameters among the properties of biodiesel by the National Petroleum, Natural Gas, and Biofuel Agency (ANP) resolutions.

CaO-NPs were used as a catalyst to produce MMEs using a transesterification method. The chromatogram in Figure 12 shows the major peaks identified. The GC-MS method employed gave a total of 7 methyl esters from MNO. Figure 12 shows the major peaks and their retention times. The 7 FAMEs identified in order of their retention times are palmitic acid methyl esters (15.94 min), linoleic acid methyl esters (18.23 min), linoleic acid methyl esters (18.29 min), steric acid methyl ester (18.62 min), linolelaidic acid methyl esters (20.25 min), linolelaidic acid methyl esters (20.85 min), and linoleic acid methyl esters (23.59 min).

The results obtained for FAMEs are similar to those reported by Taghizade [1]. The FAME results obtained from CaO-NPs are similar to those for eggshell ash. However, it was observed that the eggshell ash catalyst was more effective than CaO-NPs. The FAME obtained from CaO-NPs was less as compared to those for eggshell ash catalyst as the eggshell ash gave a total of 7 compounds, while CaO-NPs gave 7 compounds. These results are satisfactory because they confirm the suitability of chicken eggshells ash-derived CaO used as a green catalyst. Chung et al. indicated that the utilization of eggshell ash as a catalyst has less impact on the environment as compared to synthesised compounds [10].

3.2.3. Effect of Catalyst Loading. In this study, biodiesel was produced using different catalysts during the transesterification reaction: chicken eggshell ash-derived CaO and CaO-NPs. The concentration of a catalyst is a very important parameter in the production of biodiesel [80]. The conversion of biodiesel was relatively high because the biodiesel produced was above 60% from the two catalysts from the catalyst loading of 3 to 12 wt.%. The results for chicken eggshell ash-derived CaO obtained was 73%, and CaO-NPs was 53% at catalyst loading of 3 wt.%. Biodiesel yield increased with an increase in catalyst loading from 3 to 6 wt.% giving a yield of 66% for CaO-NPs. Chicken eggshell ash-derived catalyst gave a yield of 83%. The yield obtained was similar to that of Fayyazi et al. who reported a percentage yield of 81% utilizing a solid base catalyst (CaO) which was derived from chicken eggshell ash [51]. However, there was a massive drop in the yield of the chicken eggshell ash-derived catalyst beyond a catalyst loading of 6 wt.%, as the yield obtained was 64% for a catalyst loading of 9 wt.%. Wei et al. got similar results using chicken eggshell ash as a catalyst to produce biodiesel. They realized that increasing the catalyst loading to more than 10 wt.% resulted with the mixture becoming slurry or too viscous. This made it difficult for the reactants to mix and therefore, demanding more stirring power; hence, an optimum catalyst for eggshell ash was determined to be 6 wt.%. This same phenomenon was experienced with MNO [80]. Boro et al. also evaluated chicken eggshell ash catalyst incorporated with lithium to produce biodiesel in the range of

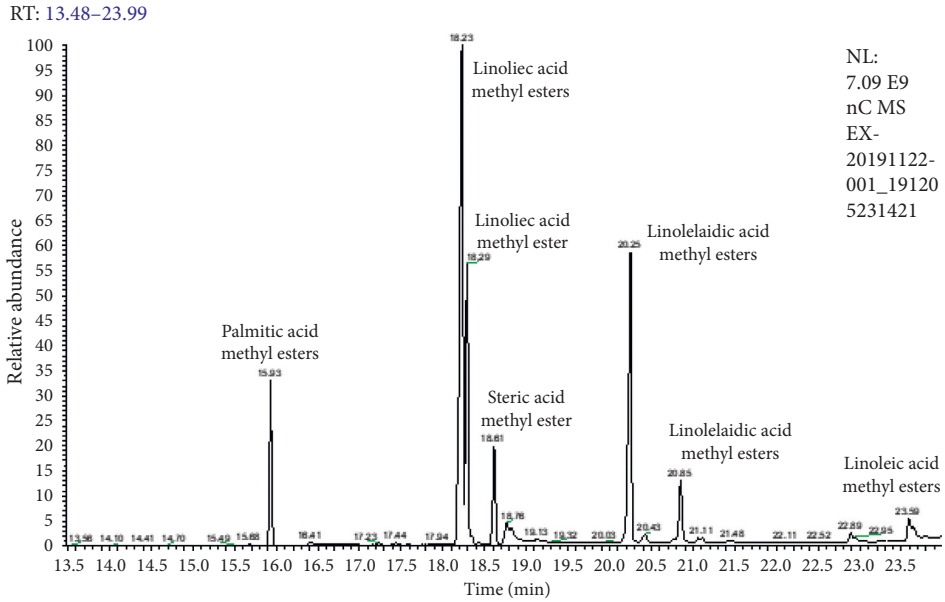

Figure 11: Chromatogram of MMEs catalyzed by chicken eggshell ash-derived CaO (refer to Supplementary Data Section 2.1).

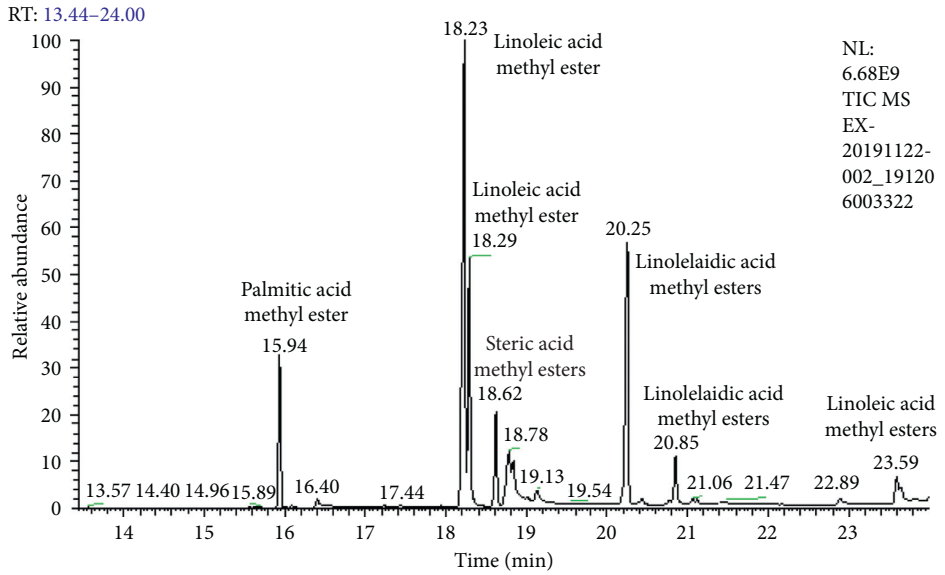

Figure 12: Chromatogram of MMEs catalyzed by CaO-NPs (refer to Supplementary Data Section 2.2).

1–8 wt.% [81]. They discovered that, beyond a catalyst loading of 5 wt.%, the conversion became constant and later dropped.

As for CaO-NPs, the yield had increased to 71% at catalyst loading of 9 wt.%. The catalyst loading was further increased to 12 wt.% and the yield for CaO-NPs increased to 85% which was highest yield recovered from CaO-NPs. Baskar et al. produced biodiesel using nanocatalysts and they discovered that, beyond a catalyst loading of 14 wt.%, the mixture became slurry and viscous which resulted in yield being reduced [82]. The optimum catalyst weight percentage for CaO-NPs was 12 wt.%, whilst the chicken eggshell ash-derived catalyst did not have any significant change, and it went a bit lower to 60%. CaO-NPs gave the highest yield of 85%. This yield was obtained from a reaction time of 3 h, temperature of 65°C, the oil to methanol ratio of 9 : 1, and a catalyst loading of 12 wt.%. The results were expected to be this way for CaO-NPs to yield the highest biodiesel since it had an estimated average crystalline size of 42 nm as compared to eggshell ash which had an estimated average crystalline size of 50 nm. In terms of catalyst loading, chicken eggshell ash-derived CaO was a better catalyst as it required a low catalyst load of 6 wt.% to obtain an optimum yield of 83% compared to CaO-NPs which obtained an optimum yield of 85% at a catalyst load of 12 wt.% However, based on these results, statistically there was no significant difference ($P > 0.05$) between CaO-NPs and eggshell (refer to Supplementary Data Section 3.1: Table 1). The results are shown in Figure 13.

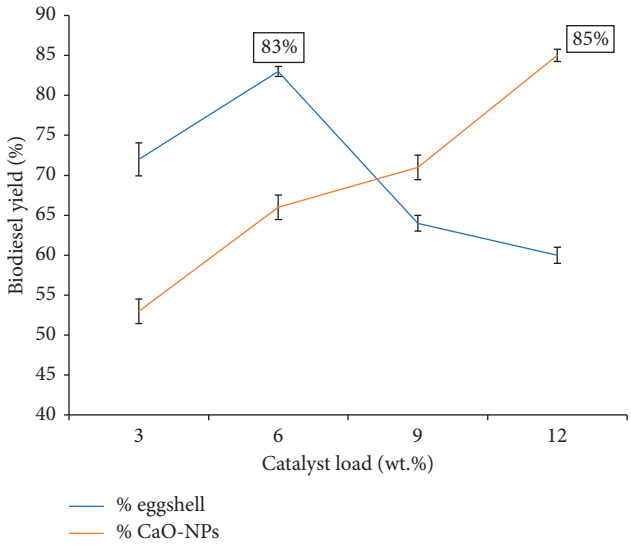

Figure 13: The effect of the amount of catalyst on the production of biodiesel.

4. Conclusions

In this study, biodiesel was produced by transesterification reaction of S*chinziophyton rautanenii* (mongongo) nut oil in the presence of a base heterogeneous catalysts: CaO derived from eggshell ash and synthesised CaO-nanoparticles (CaO-NPs). These catalysts were successfully characterized using a scanning electron microscope-energy dispersive X-ray (SEM-EDX), X-ray diffraction (XRD), and Fourier transmission-infrared (FTIR) techniques. X-ray diffraction (XRD) showed that CaO was present in both catalysts, and the average crystalline size obtained was 42 and 50 nm for CaO-NPs and eggshell ash, respectively. SEM-EDX showed agglomerated particles and high elemental composition of Ca and O for both catalysts. FTIR showed absorption bands for CaO at 875 and 713.46 cm^{-1} for CaO-NPs and eggshell ash, respectively. CaO-NPs gave a higher yield than eggshell at catalyst loading of 12 wt.% with an optimum mongongo methyl esters (MMEs) yield of 85%, while chicken eggshell-derived CaO catalyst gave an optimum MMEs yield of 83% at a catalyst loading of 6 wt.%. In terms of catalyst loading, the chicken eggshell ash-derived CaO was a better catalyst as it required a low catalyst load to obtain an optimum yield compared to CaO-NPs. However, statistically, there is no significant difference between CaO-NPs and CaO derived from chicken eggshell ash in terms of optimum yield ($P > 0.05$) using a sample t-test. The results for chicken eggshell ash-derived CaO are satisfactory more so that the average crystalline sizes are not so far off, and emphasis is on the development of environmentally friendly and suitable economical catalysts. Furthermore, the use of eggshell as a catalyst can reduce the processing cost of biodiesel, making it possible for the biodiesel to compete with diesel and fuel. The desired physicochemical properties for the produced biodiesel were within the set standards for biodiesel by European biodiesel specification (EN 1421) and American society for testing and material (ASTM D675).

Data Availability

The data can be sourced on request from the authors.

Conflicts of Interest

The authors declare that they have no conflicts of interest.

Acknowledgments

The authors are grateful to the Botswana International University of Science and Technology for funding the project and for the support by the Department of Chemistry at the University of Botswana and Botswana Institute for Technology Research and Innovation.

Supplementary Materials

1. Powder XRD characterization. 1.1. Powder XRD spectra of chicken eggshell ash-derived CaO. 1.2. Powder XRD spectra calcium oxide nanoparticle. 2. GC-MS characterization of MMEs. 2.1. GC-MS spectra MMEs using chicken eggshell ash-derived CaO. 2.2. GC-MS spectra of MMEs using calcium oxide nanoparticles. 3. Statics calculations. 3.1. Sample t-test calculations of chicken eggshell ash-derived CaO and calcium oxide nanoparticles. (*Supplementary Materials*)

References

[1] Z. Taghizade, "Determination of biodiesel quality parameters for optimization of production process conditions," Master thesis, Chemical Engineering, Polytechnic Institute of Bragança, Bragança, Portugal, 2016.

[2] I. Emeji, "Production and characterisation of biofuel from waste cooking oil," in *Proceedings of the 2015 International Conference on Chemical Engineering*, p. 18, Madras, India, August 2015.

[3] J. Ongena and G. Van Oost, "Energy for future centuries: prospects for fusion power as a future energy source," *Fusion Science and Technology*, vol. 57, no. 2T, pp. 3–15, 2010.

[4] N. Sukasem and S. Manophan, "The development of biodiesel production from vegetable oils by using different proportions of lime catalyst and sodium hydroxide," *Energy Procedia*, vol. 138, pp. 991–997, 2017.

[5] H. K. Balsora, P. Gautam, and M. K. Mondal, "Enrichment of biogas from biodegradable solid waste—a review," *Springer Proceedings in Energy*, vol. 7, no. 3, pp. 93–106, 2017.

[6] N. Cheikhyoussef, "Profiling studies of five Namibian indigenous seed oils obtained using three different extraction methods," 2018.

[7] N. Cheikhyoussef, M. Kandawa-Schulz, R. Böck, C. de Koning, A. Cheikhyoussef, and A. A. Hussein, "Characterization of *Schinziophyton rautanenii* (Manketti) nut oil from Namibia rich in conjugated fatty acids and tocopherol," *Journal of Food Composition and Analysis*, vol. 66, pp. 152–159, 2018.

[8] M. I. Al-Widyan and A. O. Al-Shyoukh, "Experimental evaluation of the transesterification of waste palm oil into biodiesel," *Bioresource Technology*, vol. 85, no. 3, pp. 253–256, 2002.

[9] N. Banerjee, R. Ramakrishnan, and T. Jash, "Biodiesel production from used vegetable oil collected from shops selling

fritters in Kolkata," *Energy Procedia*, vol. 54, pp. 161–165, 2014.

[10] Z. L. Chung, Y. H. Tan, Y. San Chan et al., "Life cycle assessment of waste cooking oil for biodiesel production using waste chicken eggshell derived CaO as catalyst via transesterification," *Biocatal. Agric. Biotechnol.*, vol. 21, pp. 101–117, 2019.

[11] K. F. Yee, J. Kansedo, and K. T. Lee, "Biodiesel production from palm oil via heterogeneous transesterification: optimization study," *Chemical Engineering Communications*, vol. 197, no. 12, pp. 1597–1611, 2010.

[12] K. Tahvildari, Y. N. Anaraki, R. Fazaeli, S. Mirpanji, and E. Delrish, "The study of CaO and MgO heterogenic nanocatalyst coupling on transesterification reaction efficacy in the production of biodiesel from recycled cooking oil," *Journal of Environmental Health Science and Engineering*, vol. 13, no. 1, pp. 1–9, 2015.

[13] S. A. Scott, M. P. Davey, J. S. Dennis et al., "Biodiesel from algae: challenges and prospects," *Current Opinion in Biotechnology*, vol. 21, no. 3, pp. 277–286, 2010.

[14] A. S. Nejad and A. R. Zahedi, "Optimization of biodiesel production as a clean fuel for thermal power plants using renewable energy source," *Renewable Energy*, vol. 119, pp. 365–374, 2018.

[15] I. M. Atadashi, M. K. Aroua, and A. A. Aziz, "Biodiesel separation and purification: a review," *Renewable Energy*, vol. 36, no. 2, pp. 437–443, 2011.

[16] A. Rajalingam, S. P. Jani, A. S. Kumar, and M. A. Khan, "Production methods of biodiesel," *Journal of Chemical and Pharmaceutical Research*, vol. 8, no. 3, pp. 170–173, 2016.

[17] N. Tshizanga, "A study of biodiesel production from waste vegetable oil using eggshell ash as a heterogeneous catalyst," M.S thesis, Chemical Engineering in the Faculty of Engineering, Cape Peninsula University of Technology, Cape Town, South Africa, 2015.

[18] M. K. Lam, K. T. Lee, and A. R. Mohamed, "Homogeneous, heterogeneous and enzymatic catalysis for transesterification of high free fatty acid oil (waste cooking oil) to biodiesel: a review," *Biotechnology Advances*, vol. 28, no. 4, pp. 500–518, 2010.

[19] O. Ogunkunle, O. O. Oniya, and A. O. Adebayo, "Yield response of biodiesel production from heterogeneous and homogeneous catalysis of milk bush seed (*Thevetia peruviana*) oil," *Energy and Policy Research*, vol. 4, no. 1, pp. 21–28, 2017.

[20] J. H. S. K. Jayamaha, *Supported Enzymes as Catalysts for Biodiesel Production*, Instituto Superior Técnico, Lisboa, Portugal, 2014.

[21] S. Singh, *Study of various methods of biodiesel production and properties of biodiesel prepared from waste cotton seed oil and waste mustard oil*, Ph.D dissertation, Thapar Institute of Engineering and Technology, Thapar University, Punjab, India, 2012.

[22] P. K. Sahoo and L. M. Das, "Combustion analysis of Jatropha, Karanja and Polanga based biodiesel as fuel in a diesel engine," *Fuel*, vol. 88, no. 6, pp. 994–999, 2009.

[23] N. S. Talha and S. Sulaiman, "Overview of catalysts in biodiesel production," *ARPN Journal of Engineering and Applied Sciences*, vol. 11, no. 1, pp. 439–442, 2016.

[24] N. Tshizanga, E. F. Aransiola, and O. Oyekola, "Optimisation of biodiesel production from waste vegetable oil and eggshell ash," *South African Journal of Chemical Engineering*, vol. 23, pp. 145–156, 2017.

[25] S. Semwal, A. K. Arora, R. P. Badoni, and D. K. Tuli, "Biodiesel production using heterogeneous catalysts," *Bioresource Technology*, vol. 102, no. 3, pp. 2151–2161, 2011.

[26] R. Romero, S. Luz, and R. Nativi, "Biodiesel production by using heterogeneous catalysts," in *Alternative Fuel*, IntechOpen Limited, London, UK, 2011.

[27] Z. Helwani, M. R. Othman, N. Aziz, J. Kim, and W. J. N. Fernando, "Solid heterogeneous catalysts for transesterification of triglycerides with methanol: a review," *Applied Catalysis A: General*, vol. 363, no. 1-2, pp. 1–10, 2009.

[28] A. H. Al-Muhtaseb, F. Jamil, L. Al-Haj et al., "Biodiesel production over a catalyst prepared from biomass-derived waste date pits," *Biotechnology Reports*, vol. 20, Article ID e00284, 2018.

[29] H. V. Lee, J. C. Juan, N. F. Binti Abdullah, R. Nizah, and Y. H. Taufiq-Yap, "Heterogeneous base catalysts for edible palm and non-edible Jatropha-based biodiesel production," *Chemistry Central Journal*, vol. 8, no. 1, pp. 1–9, 2014.

[30] T. Gebreyohans, "Production and characterization of biodiesel from Jatropha curcas seed by use K_2O/fly ash as a catalyst," M. S. thesis, Chemical and Bio Engineering, Addis Ababa Institute of Technology School of Chemical and Bio Engineering, Addis Ababa, Ethiopia, 2018.

[31] C. G. Lopresto, S. Naccarato, L. Albo et al., "Enzymatic transesterification of waste vegetable oil to produce biodiesel," *Ecotoxicology and Environmental Safety*, vol. 121, pp. 229–235, 2015.

[32] N. Kumar, "Oxidative stability of biodiesel: causes, effects and prevention," *Fuel*, vol. 190, pp. 328–350, 2017.

[33] Z.-X. Tang, D. Claveau, R. Corcuff, K. Belkacemi, and J. Arul, "Preparation of nano-CaO using thermal-decomposition method," *Materials Letters*, vol. 62, no. 14, pp. 2096–2098, 2008.

[34] Y. H. Tan, M. O. Abdullah, C. Nolasco-Hipolito, and Y. H. Taufiq-Yap, "Waste ostrich- and chicken-eggshells as heterogeneous base catalyst for biodiesel production from used cooking oil : catalyst characterization and biodiesel yield performance," *Applied Energy*, vol. 160, pp. 58–70, 2015.

[35] A. Maroyi, "Contribution of *Schinziophyton rautanenii* to sustainable diets, livelihood needs and environmental sustainability in Southern Africa," *Sustainability*, vol. 10, no. 3, p. 581, 2018.

[36] A. E. Atabani, M. Mofijur, H. H. Masjuki et al., "A study of production and characterization of Manketti (*Ricinodendron rautonemii*) methyl ester and its blends as a potential biodiesel feedstock," *Biofuel Research Journal*, vol. 1, no. 4, pp. 139–146, 2014.

[37] B. Tesfaye and A. Abebaw, "Physico-chemical characteristics and level of some selected metal in edible oils," *Advances in Chemistry*, vol. 2016, Article ID 3480329, 7 pages, 2016.

[38] K. O. Omeje, O. K. Iroha, A. A. Edeke, H. C. Omeje, and V. O. Apeh, "Characterization and fatty acid profile analysis of oil extracted from unexploited seed of African star apple (*Udara*)," *OCL—Oilseeds Fats, Crop, Lipids*, vol. 26, 2019.

[39] I. A. Ateeq, "Biodiesel viscosity and flash point determination," M. S. thesis, Faculty of Physics, Najah National University, Nablus, Palestinian, 2015.

[40] Z. Mirghiasi, F. Bakhtiari, E. Darezereshki, and E. Esmaeilzadeh, "Preparation and characterization of CaO nanoparticles from $Ca(OH)_2$ by direct thermal decomposition method," *Journal of Industrial and Engineering Chemistry*, vol. 20, no. 1, pp. 113–117, 2014.

[41] A. Lesbani, S. O. Ceria Sitompul, R. Mohadi, and N. Hidayati, "Characterization and utilization of calcium oxide (CaO) thermally decomposed from fish bones as a catalyst in the production of biodiesel from waste cooking oil," *Makara Journal of Technology*, vol. 20, no. 3, p. 121, 2016.

[42] T. Witoon, "Characterization of calcium oxide derived from waste eggshell and its application as CO_2 sorbent," *Ceramics International*, vol. 37, no. 8, pp. 3291–3298, 2011.

[43] A. M. Khan, A. H. Safi, M. N. Ahmed et al., "Biodiesel synthesis from waste cooking oil using a variety of waste marble as heterogeneous catalysts," *Brazilian Journal of Chemical Engineering*, vol. 36, no. 4, pp. 1487–1500, 2019.

[44] A. S. Balaganesh, R. Sengodan, R. Ranjithkumar, and B. Chandarshekar, "Synthesis and characterization of porous calcium oxide nanoparticles (CaO NPS)," *International Journal of Innovative Technology and Exploring Engineering*, vol. 2, pp. 2278–3075, 2018.

[45] M. Elmastaş, A. Demir, N. Genç, Ü Dölek, and M. Güneş, "Changes in flavonoid and phenolic acid contents in some Rosa species during ripening," *Food Chemistry*, vol. 235, pp. 154–159, 2017.

[46] J. Safaei-Ghomi, M. A. Ghasemzadeh, and M. Mehrabi, "Calcium oxide nanoparticles catalyzed one-step multicomponent synthesis of highly substituted pyridines in aqueous ethanol media," *Scientia Iranica C*, vol. 20, no. 3, pp. 549–554, 2013.

[47] H. R. Harsha Hebbar, M. C. Math, and K. V. Yatish, "Optimization and kinetic study of CaO nano-particles catalyzed biodiesel production from *Bombax ceiba* oil," *Energy*, vol. 143, pp. 25–34, 2018.

[48] T. Liu, Y. Zhu, X. Zhang, T. Zhang, T. Zhang, and X. Li, "Synthesis and characterization of calcium hydroxide nanoparticles by hydrogen plasma-metal reaction method," *Materials Letters*, vol. 64, no. 23, pp. 2575–2577, 2010.

[49] L. Habte, N. Shiferaw, D. Mulatu, T. Thenepalli, R. Chilakala, and J. W. Ahn, "Synthesis of nano-calcium oxide from waste eggshell by sol-gel method," *Sustain*, vol. 11, no. 11, pp. 1–10, 2019.

[50] A. Anantharaman and M. George, "Green synthesis of calcium oxide nanoparticles and its applications," *International Journal of Engineering Research and Applications*, vol. 6, no. 10, pp. 27–31, 2016.

[51] E. Fayyazi, B. Ghobadian, H. H. van de Bovenkamp et al., "Optimization of biodiesel production over chicken eggshell-derived CaO catalyst in a continuous centrifugal contactor separator," *Industrial & Engineering Chemistry Research*, vol. 57, no. 38, pp. 12742–12755, 2018.

[52] T. Zaman, M. S. Mostari, M. A. A. Mahmood, and M. S. Rahman, "Evolution and characterization of eggshell as a potential candidate of raw material," *Cerâmica*, vol. 64, no. 370, pp. 236–241, 2018.

[53] N. Tangboriboon, R. Kunanuruksapong, A. Sirivat, R. Kunanuruksapong, and A. Sirivat, "Preparation and properties of calcium oxide from eggshells via calcination," *Materials Science-Poland*, vol. 30, no. 4, pp. 313–322, 2012.

[54] N. S. W. Supriyanto, Sukarni, P. Puspitasari, and A. A. Permanasari, "Synthesis and characterization of CaO/$CaCO_3$ from quail eggshell waste by solid state reaction process," *AIP Conference Proceedings*, vol. 2120, 2019.

[55] S. Hu, Y. Wang, and H. Han, "Utilization of waste freshwater mussel shell as an economic catalyst for biodiesel production," *Biomass and Bioenergy*, vol. 35, no. 8, pp. 3627–3635, 2011.

[56] O. N. Syazwani, S. H. Teo, A. Islam, and Y. H. Taufiq-Yap, "Transesterification activity and characterization of natural CaO derived from waste venus clam (*Tapes belch*eri S.) material for enhancement of biodiesel production," vol. 105, 2017.

[57] D. K. Srivastava, A. K. Agarwal, A. Datta, and R. K. Maurya, "Horizons in internal combustion research: energy, environment, and sustainability," in *Advances in Internal Combustion Engine Research*, pp. 3–6, Springer, Singapore, 2018.

[58] C. Bhavya, K. Yogendra, K. M. Mahadevan, and N. Madhusudhana, "Synthesis of calcium oxide nanoparticles and its mortality study on fresh water fish Cyprinus carpio," *IOSR Journal of Environmental Science, Toxicology and Food Technology*, vol. 10, no. 12, pp. 55–60, 2016.

[59] D. G. Woo and T. H. Kim, "Pretreatment methods to improve the kinematic viscosity of biodiesel for use in power tiller engines," *Journal of Mechanical Science and Technology*, vol. 33, no. 8, pp. 3655–3664, 2019.

[60] B. Tesfa, R. Mishra, F. Gu, and N. Powles, "Prediction models for density and viscosity of biodiesel and their effects on fuel supply system in CI engines," *Renewable Energy*, vol. 35, no. 12, pp. 2752–2760, 2010.

[61] A. E. Atabani, A. S. Silitonga, H. C. Ong et al., "Non-edible vegetable oils: a critical evaluation of oil extraction, fatty acid compositions, biodiesel production, characteristics, engine performance and emissions production," *Renewable and Sustainable Energy Reviews*, vol. 18, pp. 211–245, 2013.

[62] C. Tsanaktsidis, K. Spinthiropoulos, G. Tzilantonis, and C. Katsaros, "Variation of density of diesel and biodiesel mixtures in three different temperature ranges," *Petroleum Science and Technology*, vol. 34, no. 13, pp. 1121–1128, 2016.

[63] E. A. Canesin, C. C. de Oliveira, M. Matsushita, L. F. Dias, M. R. Pedrão, and N. E. de Souza, "Characterization of residual oils for biodiesel production," *Electronic Journal of Biotechnology*, vol. 17, no. 1, pp. 39–45, 2014.

[64] E. P. Madus, E. C. A. Cemaluk, A. Ikechukwu Daniel, and E. V. Chinaka, "Fatty acid methyl esters of melon seed oil: characterisation for potential diesel fuel application," *Leonardo Journal of Sciences*, vol. 75–84, no. 18, pp. 75–84, 2011.

[65] B. Thangaraj, P. R. Solomon, B. Muniyandi, S. Ranganathan, and L. Lin, "Catalysis in biodiesel production-a review," *Clean Energy*, vol. 3, no. 1, pp. 2–23, 2019.

[66] P. K. Rao, S. Clarke, R. Brown, and K.-S. Wu, "Influence of iodine value on combustion and NO_x emission characteristics of a DI diesel engine," in *Proceedings of the Chemeca 2010*, Adelaide, South Australia, September 2010.

[67] N. Cheikhyoussef, M. Kandawa-Schulz, R. Böck, C. de Koning, A. Cheikhyoussef, and A. A. Hussein, "Characterization of *Acanthosicyos horridus* and *Citrullus lanatus* seed oils: two melon seed oils from Namibia used in food and cosmetics applications," *3 Biotech*, vol. 7, no. 5, 2017.

[68] M. B. Mabaleha, Y. C. Mitei, and S. O. Yeboah, "A comparative study of the properties of selected melon seed oils as potential candidates for development into commercial edible vegetable oils," *Journal of the American Oil Chemists' Society*, vol. 84, no. 1, pp. 31–36, 2007.

[69] Y. C. Mitei, J. C. Ngila, S. O. Yeboah, L. Wessjohann, and J. Schmidt, "NMR, GC-MS and ESI-FTICR-MS profiling of fatty acids and triacylglycerols in some Botswana seed oils," *Journal of the American Oil Chemists' Society*, vol. 85, no. 11, pp. 1021–1032, 2008.

[70] E. Akbar, Z. Yaakob, S. K. Kamarudin, M. Ismail, and J. Salimon, "Characteristic and composition of *Jatropha curcas* oil seed from Malaysia and its potential as biodiesel feedstock feedstock," *European Journal of Scientific Research*, vol. 29, no. 3, pp. 396–403, 2009.

[71] G. N. Anyasor, K. O. Ogunwenmo, O. A. Oyelana, D. Ajayi, and J. Dangana, "Chemical analyses of groundnut (*Arachis hypogaea*) oil," *Pakistan Journal of Nutrition*, vol. 8, no. 3, pp. 269–272, 2009.

[72] E. I. Bello and M. Agge, "Biodiesel production from ground nut oil," *Journal of Emerging Trends in Engineering and Applied Sciences*, vol. 3, no. 2, pp. 276–280, 2012.

[73] S. P. Chaurasia, A. K. Dalai, J. Gupta, and M. Agarwal, "Preparation and characterisation of Cao nanoparticle for biodiesel production from mixture of edible and non-edible oils," *International Journal of Renewable Energy Technology*, vol. 9, no. 1-2, p. 50, 2018.

[74] T. T. Kivevele and Z. Huan, "An analysis of fuel properties of fatty acid methyl ester from Manketti seeds oil," *International Journal of Green Energy*, vol. 12, no. 4, pp. 291–296, 2015.

[75] G. Kafui, A. Sunnu, and J. Parbey, "Effect of biodiesel production parameters on viscosity and yield of methyl esters: *Jatropha curcas*, *Elaeis guineensis* and *Cocos nucifera*," *Alexandria Engineering Journal*, vol. 54, no. 4, pp. 1285–1290, 2015.

[76] T. X. Nguyenthi, J. P. Bazile, and D. Bessières, "Density measurements of waste cooking oil biodiesel and diesel blends over extended pressure and temperature ranges," *Energies*, vol. 11, no. 5, 2018.

[77] Ş. Altun, F. Ya, and C. Öner, "The fuel properties of methyl esters produced from canola oil- animal tallow blends by base catalyzed transesterification," *Uluslararası Mühendislik Araştırma ve Geliştirme Dergisi*, vol. 2, no. 2, pp. 2–5, 2010.

[78] Y.-C. Juho, S.-T. Wu, T.-L. Cha, G.-H. Sun, D.-S. Yu, and C.-C. Kao, "Single session of high-intensity focused ultrasound therapy for the management of organ-confined prostate cancer: a single-institute experience," *Urological Science*, vol. 27, no. 4, pp. 226–229, 2016.

[79] A. Demirbas, "Relationships derived from physical properties of vegetable oil and biodiesel fuels," *Fuel*, vol. 87, no. 8-9, pp. 1743–1748, 2008.

[80] Z. Wei, C. Xu, and B. Li, "Application of waste eggshell as low-cost solid catalyst for biodiesel production," *Bioresource Technology*, vol. 100, no. 11, pp. 2883–2885, 2009.

[81] J. Boro, L. J. Konwar, and D. Deka, "Transesterification of non edible feedstock with lithium incorporated egg shell derived CaO for biodiesel production," *Fuel Processing Technology*, vol. 122, pp. 72–78, 2014.

[82] G. Baskar, I. Aberna Ebenezer Selvakumari, and R. Aiswarya, "Biodiesel production from castor oil using heterogeneous Ni doped ZnO nanocatalyst," *Bioresource Technology*, vol. 250, pp. 793–798, 2018.